

Raman lidar for the study of liquid water and water vapor in the troposphere

I.A. Veselovskii¹, H.K. Cha², D.H. Kim², S.C. Choi², J.M. Lee²

¹ Physics Instrumentation Center of General Physics Institute, Troitsk, Moscow reg., 142190, Russia (E-mail: katyv@orc.ru)

² Korean Atomic Energy Research Institute, P.O. Box 105, Yusong, Taejon, 305-600, Korea

Received: 4 October 1999/Revised version: 18 February 2000/Published online: 11 May 2000 – © Springer-Verlag 2000

Abstract. A Raman lidar system based on a tripled Nd:YAG laser is used for profiling of water vapor and liquid water in the troposphere. The Raman signals from water in the gas and liquid state are separated by interference filters and their relative intensities are studied for different atmospheric conditions. For clean weather or immediately after the rain the Raman signal from liquid water inside PBL is about one order of magnitude lower than the signal from water vapor. But during cloud measurements both Raman signals become comparable and the results of water vapor measurements must be corrected for the interference of liquid water Raman scattering. The obtained results are used for the estimation of liquid water content in the atmosphere.

PACS: 42.68.Rp; 93.85.+q; 94.10.Gb; 92.60.Jq

The conversion and transport of liquid water to vapor and back again is a subject of intense research. The lidars provide an unique opportunity for the atmospheric research because of the ability to monitor relatively large areas with high temporal resolution. In the last decade both DIAL and Raman systems have been successfully applied to atmospheric water studies ([1–4] and references therein). The Raman lidars, though possessing lower sensitivity as compared with DIAL systems, provide higher spatial resolution, no complicated tunable laser sources are demanded and the strong Raman line of water vapor with high frequency shift of 3657 cm^{-1} may be easily separated from elastic backscattering and Raman lines of other molecules. Raman method may be extended to include liquid water scattering. The knowledge of liquid water content is essential in physics of clouds, atmospheric photochemistry and in the study of condensation processes in polluted environments or in the presence of radioactive sources. Moreover, since the Raman contours of vapor and liquid water are partially overlapped, the bleed through of Raman signal from liquid water may introduce significant errors in vapor measurements, especially when wideband excimer lasers are used for the sounding.

Raman scattering by bulk water in the laboratory has been reported by a number of investigators [5–7], but the attempts

to apply it to atmospheric studies are not numerous. The integrated on distance Raman spectrums of liquid water and vapor excited by second harmonic of Nd:YAG laser were observed in [8] for different weather conditions. The analysis of atmospheric bulk water scattering is presented in [9, 10] where the Raman signal from liquid droplets was responsible for anomalous enhancement of water vapor contents during cloud soundings. In our paper we describe the lidar system for study of Raman scattering by liquid water and water vapor in troposphere. The obtained results allow us to compare the relative intensities of these signals for different weather conditions, to estimate the content of atmospheric liquid water, and to correct the results of water vapor measurements.

1 Experimental setup

The most intensive band in the Raman spectrum of liquid water is the valence band with wide contour which is shifted relatively to the incident radiation by the frequencies 2800 cm^{-1} – 3900 cm^{-1} . The shift of water vapor line is of 3657 cm^{-1} hence its Raman contour overlaps the liquid water contour to some degree. The small frequency interval between the Raman contours makes necessary the use of narrowband laser source for excitation. In our experiment we chose a tripled Nd:YAG laser, because 354.7-nm pumping provides sufficient efficiency of Raman process and at the same time the wavelength interval between the Raman lines makes possible the separation of Raman signals by conventional interference filters.

Figure 1 presents the shape of Raman contour of liquid water excited by 354.7-nm radiation at 20°C . The contour is calculated as a superposition of four Gaussian components. The average frequencies, half-widths of components, and their percentages for different temperatures are taken from [5]. The same picture presents the position of water vapor Raman signal and the spectral transmittance of interference filters which are used for Raman signal separation.

In our study the mobile lidar system from the Korean Atomic Energy Research Institute is used. The radiation

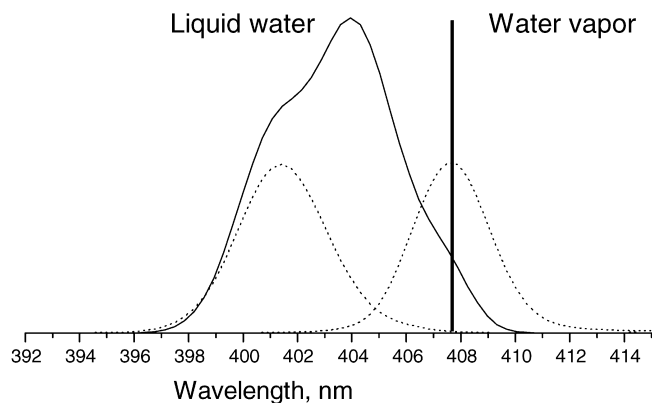


Fig. 1. The shape of Raman contour of liquid water and position of water vapor line under 354.7-nm excitation. The spectral transmittances of interference filters for Raman signals separation are shown by *dashed line*

source is tripled Nd:YAG laser of 120 mJ energy and 30 Hz repetition rate; 354.7-nm radiation is extracted from the laser output by an Abbe prism. The beam is expanded up to 50 mm and the optical axis is aligned with the axis of a 30-cm-aperture Newtonian telescope. The scanning aluminum folding mirror on the top of the van allowed us to choose the sounding direction. During the vertical measurements this mirror is removed. The telescope field of view is of 1.5 mrad, so the geometrical factor is close to unity for distances exceeding 300 m. In the spectrum analyzer the dichroic beam-splitter divides the optical signal in two channels. One channel is used for monitoring of nitrogen Raman (386.7 nm) or elastic backscatter and another one for detection of Raman signals from liquid water (401.5 nm) or vapor (407.8 nm). The change of operational wavelength in the channels is achieved by replacement of interference filters. The signals are detected by PMTs operated in analog mode and digitized by 12-bit/30-MHz ADCs. In one typical Raman measurement 10 000 laser pulses are accumulated, the obtained profiles are smoothed with 100 m averaging interval. In our two-channel system we are unable to detect all the backscattered components of interest simultaneously, so the delay between the measurements is about 10 min.

The main parameters of filters in the receiving system are summarized in Table 1. The bandwidth of the interference filters is about 3 nm. The filter for liquid water is centered

Table 1. Main parameters of filters in the receiving system

Elements	Transmission / %	Suppression of elastic signal
Interference filters:		
386.7 nm (nitrogen)	42	$> 10^8$
401.5 nm (liquid water)	12	$> 10^7$
407.8 nm (for water vapor)	29	$> 10^4$
Dielectric filter:		
386.7 nm	93	200
401.5 nm	88	
407.8 nm	88	
Semiconductor filter:		
386.7 nm	0.1	$> 10^8$
401.5 nm	14.2	
407.8 nm	21.7	

at 401.5 nm, the transmittance is 12% in the maximum and 0.15% at 407.8 nm (water vapor line). To diminish the effects related to the temperature dependence of water Raman contour, the signal monitoring near the isosbestic point at 403.7 nm is preferable [11], but for this wavelength the prevention of the bleeding throw of water vapor signal becomes more difficult. In any case the errors related to temperature variations are much smaller than the errors that originate from the uncertainty of water aerosol parameters, so at the present stage we do not take the temperature dependence of Raman contour into consideration.

One of the principal problems in Raman measurements is the suppression of elastic backscattering, which should be better than 10^{10} . In our system the demanded suppression is realized by combining the interference filters with dichroic mirrors. Dichroic mirrors possess high transmittance for Raman signals and the suppression of the pumping wavelength is around a factor of 200. In Raman channels three dichroic mirrors are installed with 1 cm separation, the mirrors are tilted at small angles to remove the reflections. The distance between the PMTs and optical filters in the spectrum analyzer is 15 cm in order to decrease the interference of possible optics fluorescence. The transmittance of liquid water channel is about 9% and suppression of elastic scattering is better than 10^{13} .

Another way to overcome the problem of elastic backscattering is the combining of interference filters with absorption edge filter. For example, the solution of hydroquinone dimethylether in ethanol is efficiently employed in lidar systems based on XeCl laser [2]. We did not find an appropriate liquid for tripled Nd:YAG laser, so we tried to use the semiconductor crystal as an edge absorber. Semiconductors have very strong absorptions for the photon energy exceeding the gap and are transparent for the longer wavelengths. The diversity of semiconductor materials allows us to choose the sample for practically any pumping wavelength. For the 354.7 nm wavelength we have chosen undoped ZnO crystal with the gap value of 3.2 eV. For the crystal of 1 mm thickness the transmittance at 407.5 nm is 21.7% and at 401.5 nm 14.2%. The transmittance for nitrogen Raman signal (386.7 nm) is smaller than 0.1%, so this filter is suited only for water Raman channel. The absorption coefficient of ZnO at 355 nm is of order of 10^4 cm^{-1} , so for a 1-mm sample the suppression value may be as high as e^{1000} . The main obstacle in realization of such high suppression is probably the emitting recombination. The efficiency of emitting channels in ZnO is expected to be quite low, but we are unable to estimate it correctly. The measurements made with thin samples demonstrate that the suppression is at least 10^8 . In our experiment we used a semiconductor filter only to verify that the elastic scattering is completely removed from the water channel and all the measurements are made with dielectric filters.

The Raman contours of water vapor and liquid water are partially overlapped, so the crosstalk between these channels is inevitable. To take the bleed throw into consideration we find the power of liquid water and water vapor Raman signals P_W , P_V from the system of linear equations:

$$P'_W = T_W(\lambda_W)P_W + T_W(\lambda_V)P_V,$$

$$P'_V = T_V(\lambda_V)P_V + T_V(\lambda_W)P_W.$$

Here $P'_{W,V}$ are signals measured in liquid water and vapor Raman channels. $T_W(\lambda)$, $T_V(\lambda)$ are the spectral transmittances of the filters in corresponding channels. The transmittance of liquid water signal $T_W(\lambda_W)$ is calculated as:

$$T_W(\lambda_W) = \frac{\int_0^{\infty} F_W(\lambda) T_W(\lambda) d\lambda}{\int_0^{\infty} F_W(\lambda) d\lambda}.$$

The bleed throw of liquid water signal in the vapor channel is described by the coefficient

$$T_V(\lambda_W) = \frac{\int_0^{\infty} F_W(\lambda) T_V(\lambda) d\lambda}{\int_0^{\infty} F_W(\lambda) d\lambda},$$

where $F_W(\lambda)$ is the shape of the liquid water Raman contour.

For our lidar $T_V(\lambda_W) = 9\%$, and the bleed throw of vapor signal in liquid water channel $T_W(\lambda_V) = T_W(407.8 \text{ nm}) = 0.15\%$.

2 Experimental results

The measurements were performed at night time during the April–May 1999 period in South Korea, Taejon. We obtained the results for different atmospheric conditions: clean weather, clouds and immediately after the rain. The typical results of vertical sounding for clean weather are presented in Fig. 2. The Raman signals from water vapor and liquid water are normalized to nitrogen Raman backscatter (P_V/P_N ; P_W/P_N). The dashed line on the same picture shows the aerosol extinction profile derived by the Klett method from the elastic signal [12]. The aerosol extinction profiles may be also obtained from nitrogen Raman backscattering. The results of comparison of these two methods we have already discussed in [13]. In our system with 30-cm-aperture

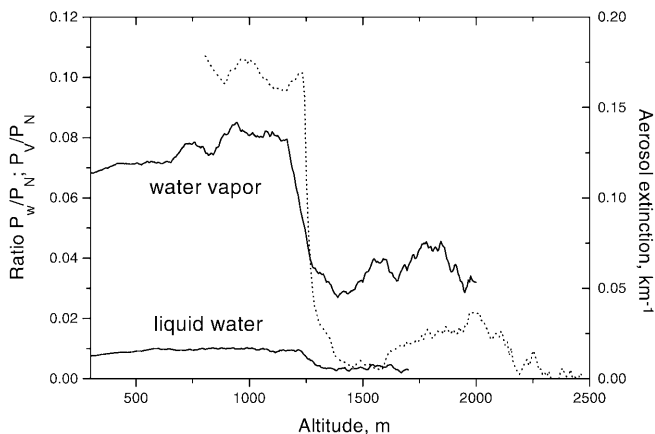


Fig. 2. Vertically measured ratio of Raman signals from water vapor and liquid water to nitrogen Raman signal (P_V/P_N ; P_W/P_N) obtained in clean weather. The dashed line shows the aerosol extinction profile derived by the Klett method. The profiles are measured with 10 min time delay

receiving mirror the Raman method may be applied with acceptable accuracy only up to 1.5 km altitude. Therefore for the data analysis we preferred to use the Klett method. The profiles in Fig. 2 are measured with a time delay of about 10 min. Above the top of the PBL which is at 1.3 km height, the concentration of both the water vapor and liquid water content sharply decreases. The mixing ratio of water vapor and liquid water is calculated from the normalized Raman signals. Neglecting at this stage the differential extinction of Raman signals, the water vapor mixing ratio n_V may be calculated as:

$$n_V = K(P_V/P_N)(\sigma_N/\sigma_N),$$

where $\sigma_{V,N}$ are the water vapor and nitrogen Raman backscattering cross sections and K is a system calibration constant. The value of K is calculated from the optical elements transmittance and from the ratio of PMTs sensitivity in Raman channels. The precision of such calibration is about 20%. The average mixing ratio of vapor inside the PBL is about $14 \pm 2 \text{ g/kg}$. The simultaneously measured temperature at 27 m height by the Environmental Engineering Group of KAERI is 25°C at a relative humidity of 85%. The corresponding water vapor mixing ratio is of 14 g/kg which is in reasonable agreement with the results of lidar measurements.

The band strength per molecule for Raman scattering by liquid water exceeds the cross section of water vapor approximately five times and is of $4.5 \pm 0.3 \times 10^{-29} \text{ cm}^2 \text{ sr}^{-1}$ [14], but the content of liquid water can not be calculated from the ratio P_W/P_N as it is done for the vapor. When the Raman scattering of spherical water droplets is considered additional factors must be taken into account: structural resonances and the shape of scattering phase function. The size distribution of atmospheric water aerosol will smooth the resonant behavior of Raman backscattering and, as demonstrated by Thurn and Kiefer [15], this effect increases the scattered intensity by approximately a factor of 2. The peaking of scattering phase function in backward direction for spheres with large radii was considered by Kerker and Druger in [16]. They found that for spheres with small size parameter $\alpha = 0.2$ the cross section will be the same as for independently scattering molecules. But for large spheres the backscattered intensity may strongly increase. The shape of phase function in [16] was calculated for refraction indices $m = 1.1, 1.5$. The change of size parameter from $\alpha = 0.2$ to $\alpha = 20$ leads to enhancement of backscattering intensity per molecule by a factor of 2 and 25 for $m = 1.1$ and $m = 1.5$, correspondingly. The authors do not provide scattering phase function for water spheres with $m = 1.33$, so we can only estimate this enhancement to be in the middle of this interval. Corresponding enhancement of Raman backscattering estimated for typical cloud water content in [9] is about 12.5–25. For our estimations we use the same values and resulting cross section of Raman backscattering is increased 25–50 times including the effect of structural resonances. So under clear sky conditions the observed liquid water content in PBL is estimated to be within the $0.006 \text{ g/kg} - 0.012 \text{ g/kg}$ interval.

During the rainy weather the measurements were made in pauses between the rain at an angle of 30° to horizon using the folding mirror. Figure 3 shows three liquid water profiles obtained on 18 May 1999. In the first measurement the small water droplets still occurred in atmosphere, so the signal was

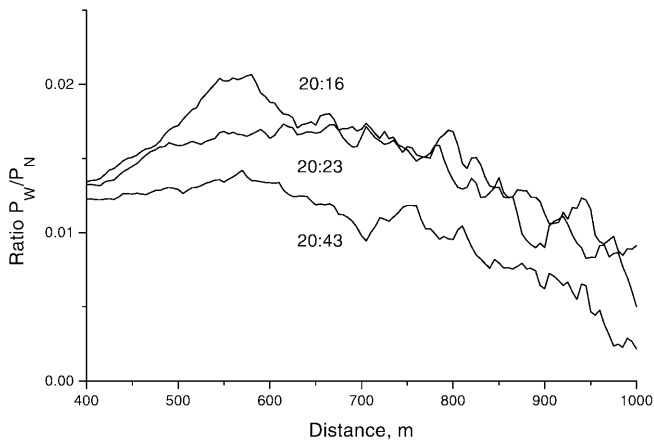


Fig. 3. Liquid water profiles obtained on 18 May 1999 immediately after rain. The sounding is produced at an angle of 30° to the horizontal

higher. To our surprise the Raman signal from liquid water after the rain was usually even smaller than for clean weather. This is probably the result of washing out of aerosol from the atmosphere.

A completely different behavior liquid water Raman signal was observed during cloudy weather. The cloud structure on May 5 is illustrated by Fig. 4 where three extinction profiles derived by the Klett method in the 19 : 35 – 21 : 45 period are presented. The extinction profiles changed rapidly, but there was always high extinction value inside the PBL and strong cloud layer at 2 km – 4 km altitudes. Figure 5 demonstrates several subsequent liquid water and water vapor vertical profiles obtained during two hours. The profiles on a picture are shifted relatively to each other on a value of 0.1. The water vertical distribution varied significantly from sounding to sounding, so the vapor profiles presented in Fig. 5 are not corrected for the water Raman signal bleed throw. The water vapor content sharply decreases at the top of PBL, the signal enhancement above 2 km correlates with the strong elastic backscattering from the cloud layers at this altitude. In contrast to vapor profiles which did not present dramatic variations with time, the behavior of liquid water signal is completely different. Initially at 20 : 18 the ratio P_W/P_N is quite small (about 0.015), but then it starts to rise inside PBL

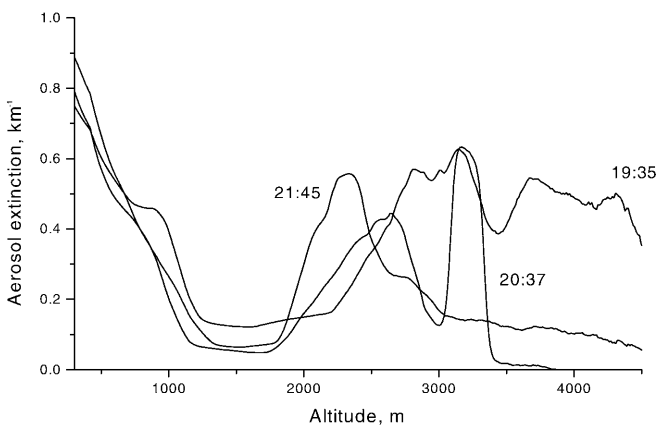
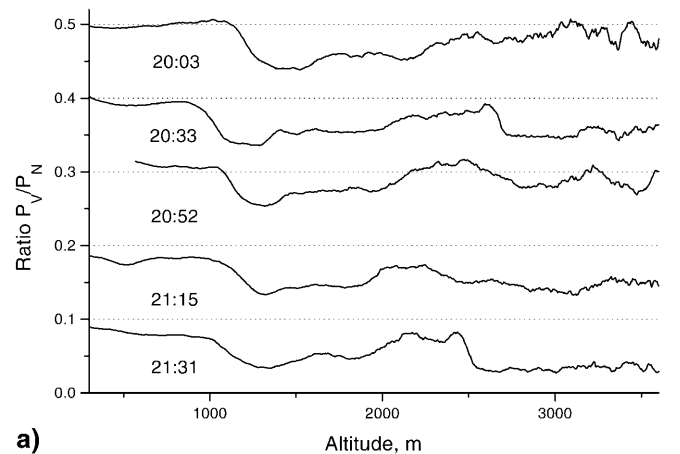


Fig. 4. Vertical profiles of aerosol extinction derived by the Klett method in 19 : 35 – 21 : 45 period on 14 May 1999

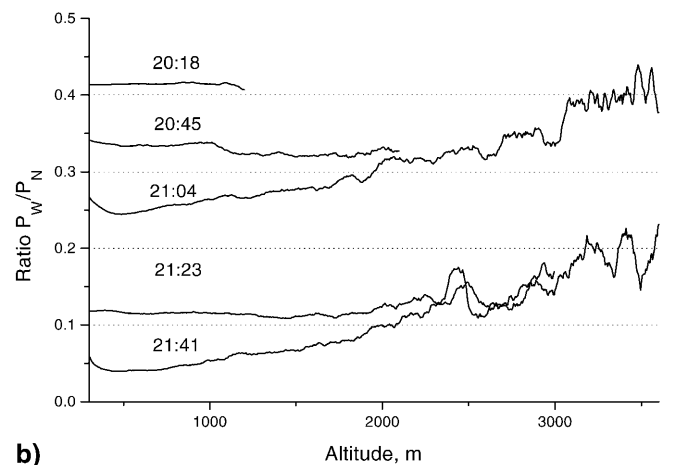
as for higher altitudes. The top of PBL is clearly visible for all vapor profiles, but at liquid water profiles it is practically absent. The behavior of vapor and liquid water signals is also completely different for high altitudes. The decreasing of the water vapor mixing ratio above 2.5 km in the 21 : 15 – 21 : 30 period corresponds to the increasing liquid water signal. The strong enhancement of Raman scattering by liquid water may originate from the cloud layers with higher water concentration. The estimation of water content in these layers leads to a value of 0.06 g/kg – 0.12 g/kg which is typical for the clouds.

The possible sources of errors in our measurements we consider to be:

- (i) Interference of elastic backscattering. To control it we inserted an additional dichroic or semiconductor filter every time when the enhanced water Raman signal was observed and compared the signal change with the mirror transmittance. During the experiment we did not find the discrepancy between these values.
- (ii) Fluorescence of atmosphere and receiving optics. The main source of atmospheric fluorescence is NO_2 , this gas is characterized by a broad fluorescent band from UV to



a)



b)

Fig. 5a,b. The ratio of Raman signals from water vapor (a) and liquid water (b) to nitrogen Raman signal obtained on 14 May 1999 during two hours. The profiles on a picture are shifted relatively to each other by a value of 0.1

IR spectral region [17]. To verify the fluorescence errors we made the measurements with another interference filter centered near 370 nm. The fluorescence of NO₂ at this wavelength is stronger than at 402 nm so the obtained value overestimates the error. The ratio of the signal to nitrogen Raman backscatter is smaller than 0.001, so at least until this ratio the results are believable.

- (iii) Stimulated Raman scattering in water droplets. Stimulated Raman scattering by water droplets requires very high intensities of 0.1 GW/cm⁻² order, thus the consideration is usually limited to spontaneous Raman scattering. The results obtained in [8] during the fog measurements demonstrate the narrowing of the spontaneous scattering spectrum, which the author attributed to stimulated scattering in droplets. In principle, when the coherent laser beam is used, the scattered Raman signal may be amplified in water droplets by the pump radiation in backward or forward direction. Our tests did not reveal any nonlinearity in the dependence of backscattered Raman signal on pump power, exceeding the measurement error, so at this stage we consider only spontaneous scattering.

Summarizing all the points mentioned above, we believe that the signals detected in our experiment originate from Raman scattering in water aerosol and the estimation of liquid water content in atmosphere is realistic.

3 Conclusion

We have separated the Raman signals from water vapor and liquid water in the troposphere and studied their relative intensities for various weather conditions. The strong signal from the liquid water is the error source during the measurements of water vapor mixing ratio in clouds. To correct this error all three Raman signals and elastic backscatter must be measured simultaneously, the corresponding four-channel spectrum analyzer is in preparation now.

The accurate estimation of liquid water content by using the Raman technique meets the significant problems. Such estimation is impossible without knowledge of water droplet size distribution. This information may be obtained from the multiwavelength sounding or by using the variable field of view lidar [18]. The additional problem is related to particles containing aqueous contribution, which needs a separate consideration. Further studies in this field, both theoretical and experimental, are demanded.

Acknowledgements. The authors gratefully acknowledge Dr. A.Z. Obidin for the suggestion to use ZnO crystal as edge absorber and preparation of the sample. We also thank Dr. D.N. Whiteman for useful comments of manuscript.

References

1. N.S. Higdon, E.V. Browell, P. Ponsardin, B.E. Grossmann, C.F. Butler, T.H. Chyba, M.N. Mayo, R.J. Allen, A.W. Heuser, W.B. Grant, S. Ismail, S.D. Mayor, A.F. Carter: *Appl. Opt.* **33**, 6422 (1994)
2. A. Ansmann, M. Riebesell, U. Wandinger, C. Weitkamp, E. Voss, W. Lahmann, W. Michaelis: *Appl. Phys. B* **55**, 18 (1992)
3. D.N. Whiteman, S.H. Melfi, R.A. Ferrare: *Appl. Opt.* **31**, 3068 (1992)
4. S.E. Bisson, J.E.M. Goldsmith, M.G. Mitchell: *Appl. Opt.* **38**, 1841 (1999)
5. J.R. Scherer, M.K. Go, S. Kint: *J. Phys. Chem.* **78**, 1304 (1974)
6. G.E. Walrafen: *J. Chem. Phys.* **47**, 114 (1967)
7. G. Schweiger: *J. Opt. Soc. Am. B* **8**, 1770 (1991)
8. O.A. Bukin: Ph.D. Dissertation, Institute of Oceanology, Vladivostok (1985)
9. S.H. Melfi, K.D. Evans, Jing Li, D. Whiteman, R. Ferrare, G. Schwemmer: *Appl. Opt.* **36**, 3551 (1997)
10. D.N. Whiteman, S.H. Melfi: Ninth ARM science team meeting proceedings, San Antonio, Texas, March 22–26, 1–6, 1999
11. D.N. Whiteman, G.E. Walrafen, W.H. Yang, S.H. Melfi: *Appl. Opt.* **38**, 2614 (1999)
12. J.D. Klett: *Appl. Opt.* **24**, 1638 (1985)
13. I. Veselovskii, B. Barchunov: *Appl. Phys. B* **68**, 1131 (1999)
14. R.B. Slusher, V.E. Derr: *Appl. Opt.* **14**, 2116 (1975)
15. R. Thurn, W. Kiefer: *Appl. Opt.* **24**, 1515 (1985)
16. M. Kerker, S.D. Druger: *Appl. Opt.* **18**, 1172 (1979)
17. J.A. Gelbwachs, M. Birnbaum: *Appl. Opt.* **12**, 2442 (1973)
18. G. Roy, L.R. Bissonnette, C. Bastille, G. Vallee: *Opt. Eng.* **36**, 3404 (1977)